Development of PRISM-FFAG Magnet

Yasushi Arimoto

Department of Physics, Osaka University

Abstract. The PRISM-FFAG magnet has been designed. The scaling condition and large acceptance of 600 mm^2 · mrad^2 has been achieved over a momentum range of 54.4 MeV/c to 81.6 MeV/c. It has been also studied influences of the air gap at connected positions in the magnet upon a magnetic field profile and a transverse acceptance.

Keywords: FFAG, Magnet, Muon
PACS: 29.20.-c

INTRODUCTION

The PRISM is a muon beam facility for the next generation, which provides a high intense, high brilliance and high purity muon beam [1, 2, 3]. The PRISM aims to search for $\mu - e$ conversion, a process beyond the Standard Model. This experiment requires a muon beam of narrow energy spread. For this purpose, a novel technique, phase rotation, is used, where low energy muons are accelerated and fast ones are decelerated by a radio frequency (RF) field.

In the PRISM, an FFAG synchrotron is used as a phase rotator and the initial momentum spread (of about $\pm$ 20 %) is squeezed down to $\pm$ 2 % [4]. During the phase rotation, tune variation must be so small that the muon beam does not cross resonance lines. This means that achromatic condition, i.e. scaling condition, is necessary. A scaling FFAG synchrotron is a good solution for this purpose. The FFAG synchrotron achieves the scaling condition by using a magnet which produces a following field profile,

$$B(r) = B_0 \left(\frac{r}{r_0} \right)^k , \tag{1}$$

here, B_0 is reference field at r_0 and r and k are, respectively, a distance from the ring center and a field index. This profile is achieved by pole shape which designed with 3D magnetic field analysis code. The detail of design will be noted later.

Since the muon beam is produced as a secondary particle, the beam emittance is very large. To achieve high intense muon beam, the acceptance of this ring should be very large. The aperture size should be about 1000 mm $\times$ 300 mm to achieve the intensity of $10^{11\sim12}$ muons/sec. The required parameters for the PRISM-FFAG synchrotron are summarized in Table 1. The magnet which meet the above requirements has been designed.

TABLE 1. Parameters of the PRISM-FFAG synchrotron

Parameter	value
Momentum acceptance	68 MeV/c $\pm$20 %
Transverse acceptance	20,000 πmm·mrad $\times$ 3,000 πmm·mrad
Equilibrium radius	6.5m @ 68 MeV/c

MAGNET DESIGN

The PRISM-FFAG magnet is a scaled-radial-sector magnet with triplet focusing and consist of three poles (DFD), and a pair of field clamp; the field clamps are equipped so as to reduce leakage of magnetic flux into RF core which located between the two magnet cells. Fig. 1 shows a perspective view of the magnet. You can refer to [5] for more detail dimension.

The design parameters which are required from a beam optics study [3] are shown in Table 2. The pole shape and magnetomotive force have been designed by iteratively calculating a 3-D magnetic field with help of a 3-D field analysis code, TOSCA (Vector-Field Co.) so as to meet the parameters.

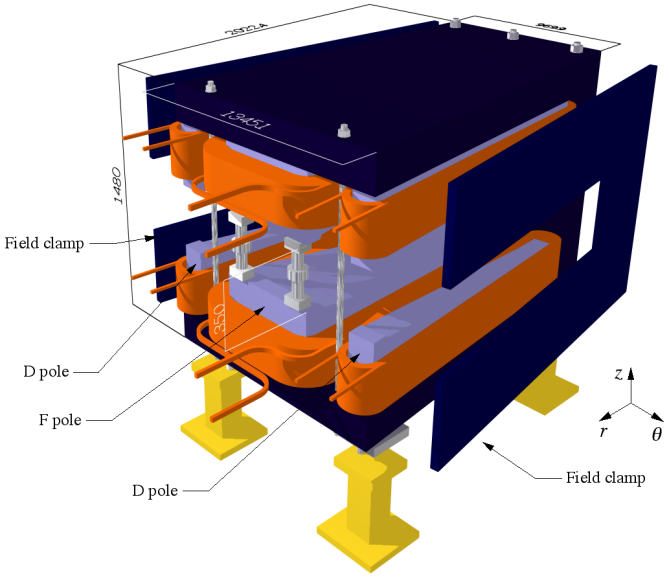

FIGURE 1. Perspective view of the PRISM magnet.

TABLE 2. Main parameters of PRISM-FFAG magnet

Parameters	values
Number of cells	10
Field index (k)	4.6
Aperture	30 cm $\times$ 100 cm
Equilibrium radius	6.5m
$B_F L$ at r = 6.5 m	0.0855 T·m/half cell
$B_D L$ at r = 6.5 m	0.0143 T·m/half cell
F/D ratio	6
Opening angle of F pole	4.4 degree
Opening angle of D pole	1.1 degree

The calculated field distributions are shown in Fig. 2, 3. Fig. 2 is an azimuthal distribution of the magnetic field at median plane. It can be seen that the direction of the magnetic field density has flipped between the F pole and D pole; this means the condition of AG focus is achieved. Fig.3 shows radial distribution of $k+1$ value and bending ratio (F/D ratio). In the left figure, the solid curve and dashed curve are respectively $k+1$ values calculated using BL integral over positive bending region and $k+1$ values calculated using that of negative bending region, and the right figure is a profile of F/D ratio plotted as a function of a radial position, a distance from the FFAG ring center. It can be seen that these values uniformly distributes over a range of 100 cm about radial position. These profiles meet requirements from the beam optics study.

PARTICLE TRACKING

Particle tracking simulations have been performed by using GEANT 3 [6]. In the simulations, muons have been tracked for 8 turns in the PRISM-FFAG ring. The vertical aperture of the ring is $\pm$15 cm and horizontal one is from $r = 565$ cm to $r = 735$ cm.

Fig. 4 shows betatron tunes plotted as a function of the muon momenta. The horizontal tunes are calculated from a betatron oscillation when the initial beam is injected at a phase space deviated by 10 mm from closed orbit in horizontal direction and at a median plane; the z and r components of the momentum are zero. The vertical tunes are calculated from a betatron oscillation when the initial beam is injected at a phase space deviated by 5 mm from median plane in

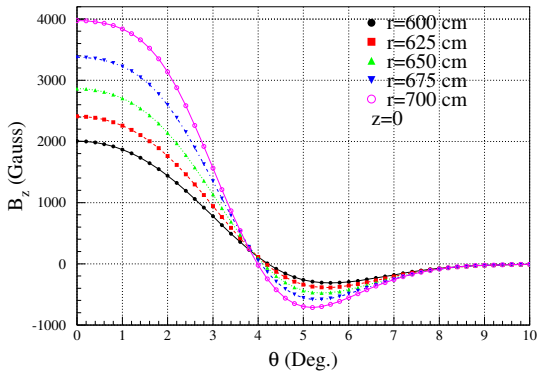

FIGURE 2. Azimuthal distribution of the magnetic field at the median plane.

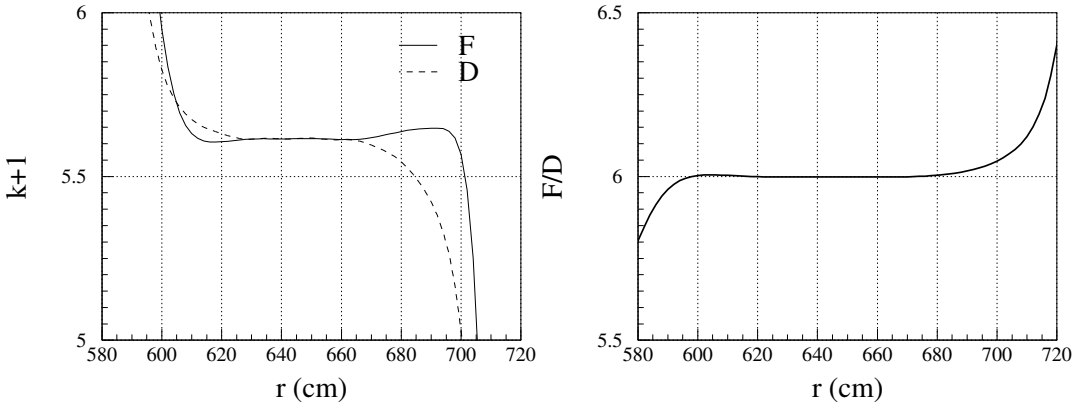

FIGURE 3. Left figure; radial distribution of k+1 value at the median plane, solid curve; k+1 value of F components, dashed curve: k+1 value of D components. Right figure; radial distribution of F/D ratio at the median plane.

vertical direction and at a closed orbit in radial direction; the *z* and *r* components of momentum are zero. It is found that the horizontal and vertical tunes does not vary over the momentum range from 54.4 MeV/*c* to 81.6 MeV/*c*.

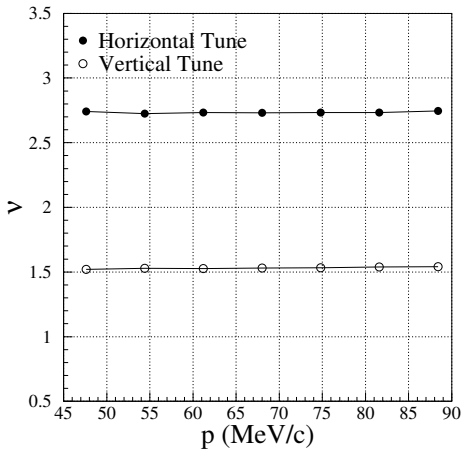

FIGURE 4. Betatron tune as a function of muon momenta. Closed circles: Horizontal tune. Open circles: Vertical tune.

To evaluate a transverse acceptance in 4D phase space, 4D tracking has been carried out. In the 4D tracking , the initial beam is uniformly distributed in 4 D phase space while the momentum is fixed. The acceptance is defined by a volume of an initial 4D-transverse-phase-space at a center of a straight section where particles survive after 8 turns

tracking. The simulation results of the 4D acceptance are shown in Fig. 5 as a function of the muon momentum. The 4D acceptance of 6.0×10^8 mm^2·mrad^2 has been achieved at 68 MeV/c. This value is approximately same as an aimed 4D acceptance as shown in Table 1. It has been found that the acceptance does not vary over the momentum range of 54.4 to 81.6 MeV/c which corresponds to a momentum range of $\pm$ 20 %.

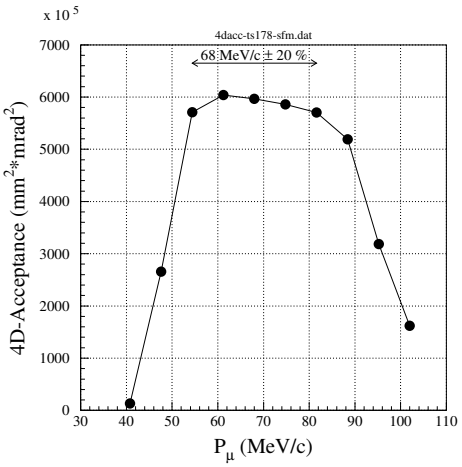

FIGURE 5. 4D transverse acceptance as a function of muon momenta.

INFLUENCE OF AIR GAP

Yoke structure

The PRISM-FFAG magnet is divided into two parts at median plane. The upper (or lower) yoke consists of 6 constructional members (Fig. 6). This configuration provides good cost performance because the yoke is able to be produced from not iron block but iron plates (if you produce the magnet from iron block, the yoke should be proceeded a forging).

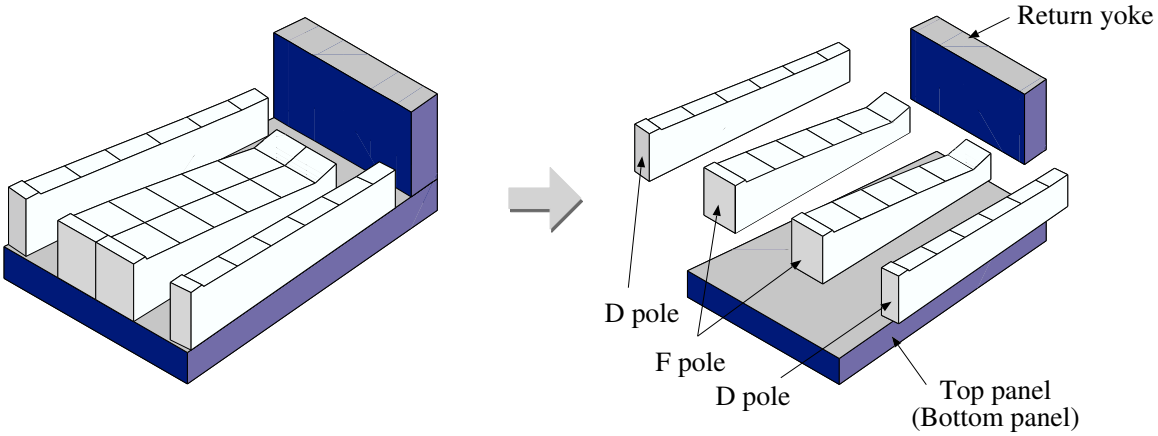

FIGURE 6. Yoke structure

Influence of air gap at connected point in the yoke

The structure which consists of several pieces make a thin air gap at each connected position due to machinery error. By using the 3D calculation code, TOSCA, it has been studied how much the gaps have an influence on the field

profile of the magnet. In a model of the calculation, the air gap layer is inserted at a connected position between a top panel and a return yoke as shown in Fig. 7.

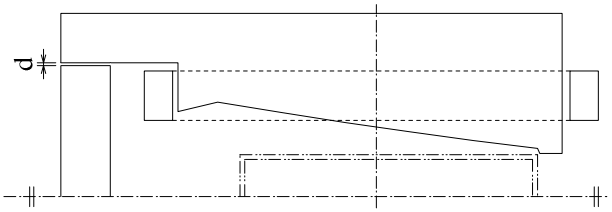

FIGURE 7. Position of the air gap (indicated by “d”).

Fig. 8 shows the air gap dependence of a deviation of *BL* integral from ideal one defined by

$$\delta = R_{BL} - 1, \tag{2}$$

$$R_{BL} = \frac{BL}{BL_0}, \tag{3}$$

where BL and BL_0 are respectively, BL integral of a magnet which has the air gap and an ideal magnet which has no air gap. Solid curves and dashed curves are respectively δ of F components and D components. It can be seen that the δ of D components increase as the air gap increases, on the other hand, F components decrease. This behavior can be explain as flows; the flux of the F pole produced by that of the main coil flows along two path. On the first path, the flux starts from the F pole and flow into the return yoke via top panel and goes to lower F pole via a bottom panel. On the second path, the flux started from the pole flows into the D poles via the top panel and goes to the lower D pole via median plane and flows into the lower F pole via the bottom panel. When the air gap is inserted to the return yoke, the magnetic resistance of the former path increases and that of the latter one relatively decreases. As the results, the magnetic flux from the F pole flows into the D pole increases and then the BL integral of the D components increase.

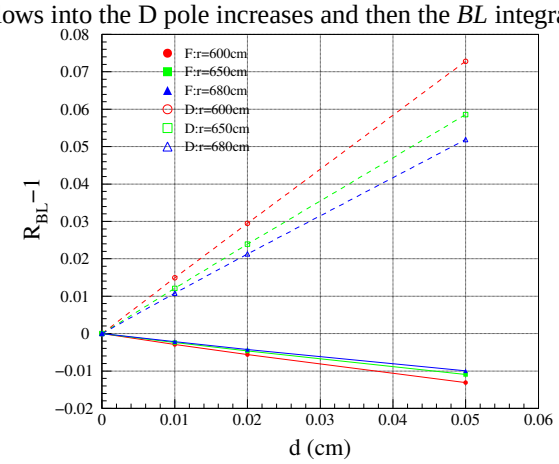

FIGURE 8. Deviation of BL integral from ideal magnet. as a function of the air gap at the return yoke.

To estimate influences of the error from the magnetic profile on 4 D acceptance, the tracking simulation has been performed. Since it can bee seen from Fig. 8 that the value of δ about the D component is much larger than that of the F one, the simulation has been demonstrated by including error of only D components. In the simulation, 10 magnets consisted of three different magnets in field profile of D component are set in the FFAG ring. These different magnets have been created by changing current of D main coils. The current of the three coils has been set as follows,

- Magnet ♯1: I_D=I_0,
- Magnet ♯2: I_D=$(1+R/100)I_0$,
- Magnet ♯3: I_D=$(1-R/100)I_0$.

The results of the tracking are shown in Fig. 9. The Fig 9 is 4-D acceptance plotted as a function of the deviation of BL integral of the D component from the ideal magnet, δ. The tracking has been carried out with three kind of magnets layout in the ring. In the first ring, the magnets are put in order of 1-1-2-2-3-3-1-2-3-1, here, the numbers

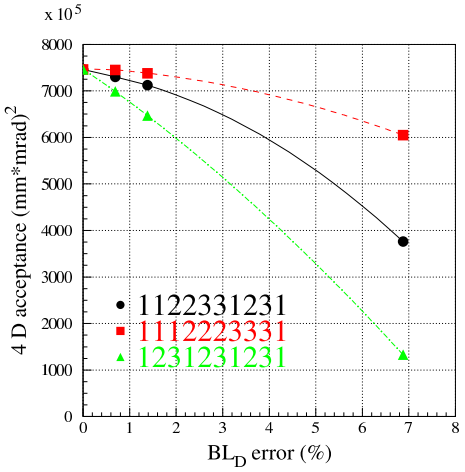

FIGURE 9. 4D acceptance variation as a function of the error of the *BL* integral of the D component.

indicate the magnet number listed above. In second one, the magnet are put in order of 1-1-1-2-2-2-3-3-3-1, and in third one, are put in order of 1-2-3-1-2-3-1-2-3-1. If we accept the reduction of 10 % in 4-D acceptance, acceptable error of BL_D is less than ± 0.7 %. This corresponds to 1.4 % deviation of δ due to the air gap at the return yoke (the thickness of air-layer-gap never become less than 0 so the error tolerance of ± 0.7% correspond to from 0 to $+1.4$%). From Fig. 8, it can bee seen that a tolerance of the air gap is less than 0.1 mm. This accuracy can be easily achieved in a manufacturing.

Influence of air gap at connected point of field clamp

The RF core of the PRISM-FFAG cavity is made from magnetic alloy, FINEMET (Hitachi Co.). The FINEMET is high-permeability material; (relative magnetic permeability is more than 200,000) so the RF core indraw a leaked magnetic field from the FFAG magnet. If the magnetic field density in the RF core exceed a few hundred Gauss, the relative permeability (of complex term in parallel expression) of the RF core will degrades and an impedance of the RF cavity is reduced [7].

To avoid this situation, the field clamp has been installed between the magnet and the RF core, where the leaked flux flows into the clamp and the RF core in a ratio of the magnetic resistance of a path via the clamp and that of via the RF core. Since the path via the RF core passes more air gap than the clamp, the flux almost flows into the clamp.

However, the field clamp is divided to two parts at a median plane as shown in Fig.10. The ratio of the magnetic flux flows into the RF core to that of the clamp increases as the magnetic resistance of the field clamp increases due to an air gap at the connected position.

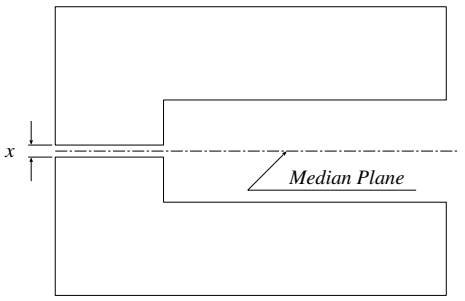

FIGURE 10. Inserted gap position at the field clamp

Influences of the air gap on the magnetic flux in the RF core has been studied by TOSCA. In Fig. 11, contour plot of magnetic field density in the RF core are shown; the left figure is the plot calculated with no air gap clamp and the

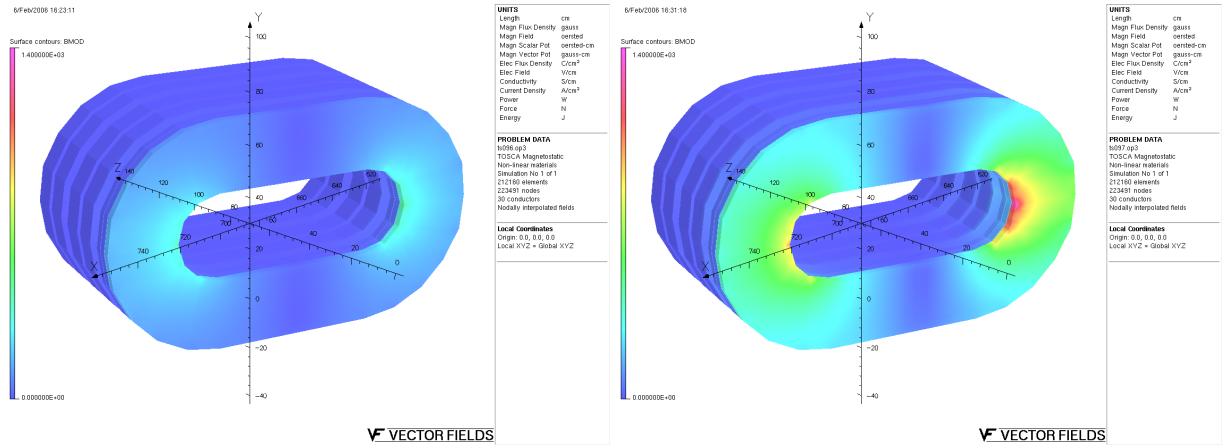

FIGURE 11. Contour plot of magnetic flux density in the RF core. Left: no air gap inserted at a connected position of a field clamp. Right: 1 mm gap inserted at the connected position of the filed clamp.

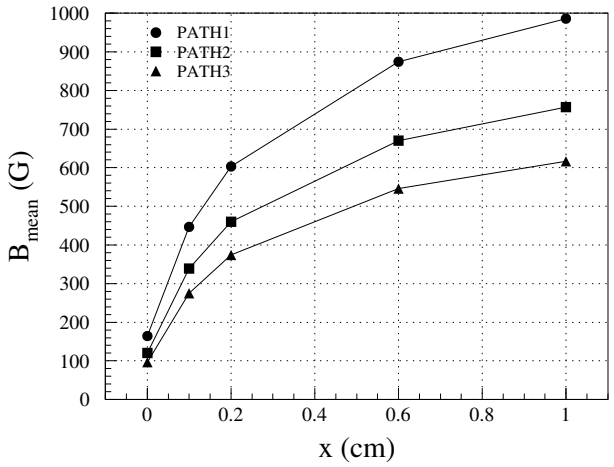

FIGURE 12. The air gap dependences of mean magnetic flux density in the RF core.

right figure is that with the clamp with an air gap of 1 mm at a connected position(Fig. 10). In case of 1 mm air gap, the field flux in the RF core is more than 3 hundred Gauss.

Fig. 12 shows the average magnetic flux at the RF core integrated along racetrack perimeters as a function of the air gap, *x*, at the connected position of the clamp. Path 1 is an inner racetrack perimeter, and path 2 is a center perimeter and path 3 is an outer perimeter. From Fig. 12, it is found that the machinery accuracy of the air gap of less than 0.1 mm is necessary to suppress the flux less than a few hundred Gauss. It is difficult to assemble the clamp by such a precision. So we select the method to nip the field clamp from both side with two iron plates at the connected position. Even if the air gap is produced at the connected point of the upper clamp and the lower clamp, the flux flows from the upper clamp to the lower one via the side plates.

SUMMARY

The design of the PRISM-FFAG magnet has been completed. From the particle tracking simulation using GEANT3, it has been given that the scaling condition of beam orbit has been established and the 4D transverse acceptance of 6×10^6 mm^2·mrad^2 has been achieved in the FFAG ring which consists of the designed magnet .

It has been shown that the tolerance of the air gap at connecting point in the yoke is less than 0.1 mm from the 3-D field analysis and the tracking simulations including the field error of D component,

It has been found that the gap at connected point at the field clamp is sensitive to magnetic flux leaked into the RF core. To reduce the flux leakage, the two iron plate has been attached at the connected point of the filed clamp.

ACKNOWLEDGMENTS

This project has been supported by Grant-in-Aid for Scientific Research of Japan Society for the Promotion of Science.

REFERENCES

1. The PRISM project – A Muon Source of the World Highest Brightness by Phase Rotation –,LOI for Nuclear and Particle Physics Experiments at the J-PARC (2003).
2. Y. Kuno, "High Intensity Muon Beam Facilities with FFAG," in *Proceedings of the Particle Accelerator Conference (PAC2005)*, Knoxville, Tennessee, 2005, pp. 29–33.
3. A. Sato, M. Aoki, Y. Arimoto, Y. Kuno, Y. Kuriyama, T. Matsushima, K. Nakahara, S. Nakaoka, M. Yoshida, M. Aiba, S. Machida, Y. Mori, C. Ohmori, T. Yokoi, M. Yoshimoto, K. Yoshimura, Y. Iwashita, N. Sasao, and S. Ninomiya, "Design and Construction Status of an FFAG for the PRISM Project," in *Proceedings of The 17th International Conference on Cyclotrons and Their Applications, Cyclotrons 2004*, 2004, pp. 235–237.
4. Y. Kuriyama, *to be published in Nuclear Physics B, Proceedings Supplements* (2006).
5. Y. Arimoto, M. Aoki, Y. Kuno, Y. Kuriyama, T. Matsushima, K. Nakahara, S. Nakaoka, A. Sato, M. Yoshida, Y. Iwashita, M. Aiba, S. Machida, Y. Mori, C. Ohmori, T. Yokoi, M. Yoshimoto, K. Yoshimura, and S. Ninomiya, "Study of the PRISM FFAG Magnet," in *Proceedings of The 17th International Conference on Cyclotrons and Their Applications, 'Cyclotrons 2004'*, 2004, pp. 243–245.
6. Application Software Group Computing and Networks Division, *GEANT, Detector Description and Simulation Tool*, CERN (1994).
7. C. Ohmori (2003), private communication.